Prophages regulate *Shewanella fidelis* 3313 motility and biofilm formation: implications for gut colonization dynamics in *Ciona robusta*

Ojas Natarajan[1], Susanne L. Gibboney[1], Morgan N. Young[1], Shen Jean Lim[4], Natalia Pluta[2*], Celine G.F. Atkinson[3], Brittany A. Leigh[1,4*], Assunta Liberti[1,5], Eric D. Kees[7**], Mya Breitbart[4], Jeffrey A. Gralnick[6,7], and Larry J. Dishaw[1,3,4‡]

[1.] Morsani College of Medicine, Pediatrics, [2]Biomedical Sciences Program, [3]Department of Cell Biology, Microbiology, and Molecular Biology, [4]College of Marine Science, University of South Florida, Tampa, Fl USA, [5]Stazione Zoologica Anton Dohrn, Naples, Italy, [6]Plant and Microbial Biology, University of Minnesota, USA, [7]BioTechnology Institute, University of Minnesota, USA.
* Current address: LifeSci Communications, New York and Boston, USA.
** Current address: Cargill Corporation, Wayzata, MN, USA.
‡ Corresponding author: ldishaw@usf.edu

Abstract

Prophages are viruses that integrate into the genomes of bacteria, which then become lysogens. Lysogens are abundant in the gut of animals, where prophages are known to influence their metabolic pathways and other traits. However, the potential influence of prophages on the gut microbiota-host immune axis in animals remains poorly understood. Here, we investigated the influence of prophages in a marine lysogen, *Shewanella fidelis* 3313, a prevalent member of the gut microbiome of the model tunicate, *Ciona robusta*. Two prophages, SfPat and SfMu1, were deleted individually and in combination using homologous recombination to observe the effects of these prophages on processes involved in gut colonization. We report here that *in vitro*, these prophages enhance motility and negatively impact biofilm formation of *S. fidelis* 3313. To understand the *in vivo* impact of these prophage-induced changes in bacterial traits, we exposed metamorphic stage 4 *Ciona* juveniles (the stage that correlates to first feeding and subsequent gut colonization) to both wildtype (WT) and modified strains of *S. fidelis* 3313. When colonizing the *Ciona* gut, the WT strain experiences an upregulation of *pdeB*, a phosphodiesterase known to degrade cyclic di-

GMP, a dinucleotide messenger that can positively influence biofilm formation while negatively regulating motility. WT colonization and upregulation of *pdeB* also correlates to a downregulation of the *Ciona* gut immune effector, VCBP-C. This study reveals an influence of prophages on bacterial traits and host immune response in the gut of a model organism. Our findings highlight the importance of interkingdom signaling between prophages, bacteria, and their animal hosts in regulating the gut microbiota-host immune axis.

Introduction

The gastrointestinal tract (or the gut) of animals is lined by an epithelial layer with a mucus-rich surface; this environment is dynamic and serves as a primary interface between host immunity, symbiotic microbes, and dietary antigens [1, 2]. In the process of colonizing the gut, bacteria encounter physical, chemical, and biological forces. They must compete for nutrients and niche space while managing the stress of digestive enzymes and host immune factors [3-6]. Gut colonizing bacteria often also encounter bacteriophages, or viruses that infect bacteria [7], with over 10^{12} viruses expected to reside in the human gut [8].

Bacteriophages (phages) can exist as lytic or temperate viruses. Conventionally, temperate phages integrate into bacterial genomes as prophages and remain ‘dormant’ until an external trigger activates them to enter the lytic cycle [9-11]. Bacteria containing prophages are considered to be ‘lysogenized’ and referred to as lysogens [9, 10]. Prophages often encode accessory genes that can influence bacterial traits and behaviors [12]; these genes include virulence factors, antibiotic resistance genes, and those that provide superinfection exclusion, thereby protecting their bacterial hosts from

infections by related phages [13]. Based on the site of integration, prophages can also impact the expression of bacterial genes [14]. Bacteria that carry prophages exist in every environment [15-17] and the microbiomes of diverse animals include a large proportion of lysogenized bacteria [8, 18]; e.g., it has been reported that 48-72% of murine gut bacteria contain prophages [18].

Induction of prophages among lysogenic bacteria can result in lysis and can be mediated by a variety of stressors, including antibiotics and inflammatory processes [19-27]. Because prophages can influence the phenotypes of their bacterial hosts, such as biofilm formation [25], understanding the impact of lysogenized bacteria in animal microbiomes is becoming a research priority [28-30]. In the gut, microbial aggregates like biofilms may benefit the host by enhancing physical barriers against pathogenic invasion [31]. In *E. coli* K-12, the integration of Rac prophage into the host's tRNA thioltransferase region disrupts biofilm functions [32]. Deletion of this prophage decreased resistance to antibiotics, acids and oxidative stress. These traits are likely encoded by specific prophage genes [26], influencing biofilm formation and affecting motility. Prophages are also known to shape biofilm lifecycles in *Pseudomonas aeruginosa* and *Shewanella oneidensis* [33, 34].

Lysogenic bacteria from the genus *Shewanella* colonize *Ciona robusta*, an ascidian collected in Southern California waters [35, 36] and from here on referred to as *Ciona*. Tunicates like *Ciona* are a subphylum (Tunicata) of Chordates that are well-established model systems for studies of animal development [37-39], and are now increasingly leveraged for gut immune and microbiome studies [40]. Although *Ciona* only possesses innate immunity, it can maintain stable gut bacterial and viral

communities [17, 35] despite continuously filtering microbe-rich seawater. Previous efforts to define gut immunity in *Ciona* revealed the presence of a secreted immune effector, the variable immunoglobulin (V-Ig) domain chitin-binding protein, or VCBP, that likely plays important roles in shaping the ecology of the gut microbiome by binding bacteria and fungi (as well as chitin-rich mucus) on opposing functional domains [41, 42]. VCBP-C is one of the best-studied VCBPs expressed by *Ciona* in the stomach and the intestine, and it has been shown to bind bacteria *in vitro* and in the gut lumen [42]. It was proposed, based on a variety of *in vitro* and *in vivo* observations, that VCBPs likely modulate bacterial settlement and/or biofilm formation [40, 41, 43]. The potential influence of soluble immune effectors on host-bacterial-viral interactions is of considerable interest. However, the possibility that prophages influence how VCBP-C interacts with or recognizes bacteria has not been explored.

We previously isolated *Shewanella fidelis* strain 3313 from the gut of *Ciona*, and discovered two inducible prophages, SfPat and SfMu [36], the latter of which is recognized as SfMu1 in the current manuscript. Furthermore, *in vitro* experiments demonstrated enhanced biofilm formation in *S. fidelis* 3313 in the presence of extracellular DNA that could originate from lytic phage activity [36]. The link between phage-mediated lysis and biofilm formation has previously been demonstrated in other *Shewanella* species [34]. For example, in *Shewanella oneidensis* strain MR-1, Mu and Lambda prophages enhanced biofilm formation via extracellular DNA (eDNA) released during prophage-induced lysis, where the genomic DNA likely served as a scaffold for biofilms [34]. Similarly, the P2 prophage of *S. putrefaciens* strain W3-18-1 influenced

biofilm formation via spontaneous induction at low frequencies, resulting in cell lysis and contributing eDNA that can support or help mediate biofilm formation [44].

Here, we set out to characterize the influence of prophages, SfPat and SfMu1, on their host, *S. fidelis* 3313. The genome assembly for *S. fidelis* 3313 was further improved by combining both long-read and short-read sequencing, resulting in improved resolution of the genomic landscape of the prophages and associated regions. We then designed a homologous recombination-based deletion strategy to generate sub-strains with one or both prophages deleted, i.e., knocked-out. We report that the genetically modified sub-strains exhibited reduced motility and increased biofilm formation *in vitro*, behavioral changes detectable by gut immunity and resulting in altered VCBP-C expression patterns. Colonization of the gut of laboratory-reared *Ciona* juveniles with prophage knockout (KO) or wild-type (WT) strains suggests that the influence of prophages on bacterial colonization of the gut is impacted by host genetics. The results of this study reflect on complex transkingdom interactions among prophages, their bacterial hosts, and animal immune systems.

Methods

Culture and growth conditions

Shewanella fidelis 3313 used in this study was originally isolated from the gut of *Ciona robusta* obtained from Mission Bay CA USA, as previously described [36]. The bacterium was cultured in Difco marine agar 2216 (MA) (Fisher Scientific, Hampton, NH) and marine broth (MB) at room temperature. Subsequent genetic manipulations

were performed on strains grown in a mixture of 75% LB (Lysogeny Broth, Fisher Scientific, Hampton, NH) and 25% MB (LB/MB).

Genome Assembly

Metagenomic libraries were prepared from isolated colonies on marine broth using NuGen Ovation Ultralow DNA kit (Eurofins, Louisville KY) for Illumina sequencing and SMRTbell II for Pacbio sequencing. Samples were sequenced on the Illumina MiSeq 2x250 bp platform (San Diego, CA, USA) and PacBio SMRTcell (Pacific Biosciences, Menlo Park, CA, USA). Illumina-sequenced reads were quality-trimmed at Q=30 with Trimmomatic v0.36 [45] and co-assembled with PacBio-sequenced reads using Unicycler v0.4.8 [46]. Genome completion, strain heterogeneity, and contamination were assessed using checkM v1.0.9 [47]. Whole genome amino acid identity (AAI) was used to identify or verify taxonomy using compareM v0.0.2.3 [48]. The assembled genome was annotated by the Rapid Annotation using Subsystem Technology (RAST) server [49]. Identification and annotation of prophage-encoding genome regions was performed with a software pipeline that included PhiSpy [50], VirSorter, PHASTER and VIBRANT [51-53].

Prophage deletion

Two prophages, SfPat and SfMu1, were targeted for deletion from *S. fidelis* 3313 using homologous recombination to produce single and double knockout sub-strains. First, a pSMV3 suicide (or deletion) vector [54] was designed with ≈700 bp regions corresponding to the upstream and downstream sequence of the prophages. These flanking regions were amplified and ligated using overlap extension PCR, then

directionally inserted into the vector with the restriction enzymes BamHI and SacI [55]. Plasmid conjugation was then performed by inoculating a colony of *S. fidelis* 4066 into a culture of *E. coli* containing the desired suicide vector on a LB/MB agar plate for two hours.

Plasmid inserts containing the flanking regions of the prophage, a kanamycin resistance selection marker (Kan^R), and a sucrose sensitivity marker (*sacB*) were integrated into the genome of *S. fidelis* via homologous recombination. Successful conjugants were isolated on LB/MB with 200 µg/ml kanamycin plates at room temperature (RT). Conjugants were confirmed by PCR screening and grown to turbidity in LB/MB broth with kanamycin. The cultures were then serially diluted, streaked onto LB/MB + 10% sucrose and incubated overnight at RT to encourage plasmid excision via SacB counter-selection. This second round of homologous recombination leads to two possible outcomes: excision of the prophage with the plasmid, or excision of only the plasmid leaving the prophage intact in the genome. Colonies lacking the prophage were identified by screening for flanking regions on either side of the prophage. For example, excision of the prophage is expected to result in a 1.4 kb PCR product that corresponds to sequences flanking the prophage SfMu1.

TEM visualization of prophages

S. fidelis 3313 was grown to log phase in 3 ml of MB for 4 hrs at RT. Three microliters of the 1 mg/ml mitomycin - C stock was added to the log phase bacteria for induction, followed by overnight shaking at RT [56]. Induced samples were then spun down and the supernatant was 0.22 µm filter-sterilized, and a sucrose cushion

centrifugation was performed using 38% sucrose in SM buffer at 17500 xg for 3 hrs and 45 mins at 15 ^{o}C [57]. Pelleted samples were resuspended in 500 µl of 20 nm filter-sterilized SM buffer. The phage particles were prepared for TEM imaging on carbon coated 200 square mesh copper grids. The samples were negatively stained and observed using JEOL JEM1400 operated at 80 Kv and equipped with a Gatan OriusSC1000 digital camera [58].

S. fidelis crystal violet biofilm assay

WT and prophage KO strains were cultured in MB overnight at RT, and then diluted to 10^7 cfu/ml in MB with or without the immune effector, VCBP-C (at 50 µg/ml) [43]. The cultures were brought to 2 ml final volume of MB in 12-well dishes and incubated at RT for 24 hrs to examine biofilm development. Each variable was tested in technical duplicate. Biofilms were quantified by crystal violet staining as previously described [59]. Briefly, supernatants were aspirated after 24-hour incubation and the biofilms were dried and stained with 0.1% crystal violet for 10 mins. The stained biofilms were then gently washed with deionized water, and the amount of biofilm produced was quantified as the intensity of stain extracted with 30% acetic acid for each well and measured via optical density at 570 nm. All biofilm assays were performed in triplicate.

Motility assay

To compare swimming behaviors, soft-agar overlay motility assays were performed in 12-well dishes [60, 61]. A bacterial colony was cultured overnight at RT and then inoculated onto the center of soft agar (containing LB/MB and 0.5% low-melt

agarose). The plates were incubated at RT overnight and results were recorded as the distance traveled (in millimeters) from the inoculation zone. Each variable was tested in duplicate. Two perpendicular distances (from the inoculation zone) were recorded and averaged for each well.

Ciona mariculture

The *in vivo* colonization experiments were performed on animals reared under conditions termed “semi-germ-free” (SGF), which include minimal exposure to marine microbes. SGF conditions include animals harvested under conventional approaches [62] but permanently maintained in 0.22 µm-filtered, conditioned artificial seawater (cASW), handled with gloves, and lids only carefully removed for water/media changes. cASW is prepared by conditioning artificial sea water made with Instant Ocean™ in an in-house sump-aquarium system containing live rock and growth lights along with sediment from San Diego, California; salinity is maintained at 32-34 parts per thousand (or grams per liter). Compared to germ-free [63] or conventionally-reared (CR) approaches, CR includes a step-up exposure to 0.7 µm-filtered cASW that introduces marine bacteria more naturally. The SGF approach is considered an intermediate method of rearing that includes minimal microbial exposures while increasing developmental maturity (unpublished observations). The animals were reared at 20 ^{o}C from larval to juvenile stages. Since *Ciona* are obtained from Mission Bay to generate juveniles for each of the biological replicates, the animals offer wider genetic diversity than conventional models like laboratory mice, *Drosophila* and *Caenorhabditis elegans*, which are usually genetically tractable.

Gut colonization assays

All strains were grown overnight at RT in MB and diluted to 10^7 cfu/ml in cASW after repeated washes. Metamorphic stage 4 (MS4) animals reared in six well dishes in cASW were exposed to five ml of 10^7 cfu/ml bacteria in each well for one hour. MS4 animals are considered part of the 1st ascidian stages (post-settlement stages 1-6, whereas stage 7-8 and onwards are 2nd ascidian stages, and reflect young adult animals) and can be identified as having a pair of protostigmata, or gill slits, on each side of the animal [37]. MS4 animals first initiate feeding via newly developed and opened siphons; prior to this, the gut remains closed and the inside lumen is unexposed to the outside world, or sterile. Following this initial exposure, or colonization, the plates were then rinsed multiple times with cASW and replaced with fresh cASW. Ten juveniles were chosen at random for each treatment, pooled, and homogenized with a plastic pestle; live bacteria were counted by performing serial dilutions and enumerating colony forming units (cfu) via spot-plating assays [64, 65]. Each graph represents a biological replicate dataset from genetically distinct/ diverse backgrounds of *Ciona* (represented by separate live animal collection and spawning events). Statistical significance was calculated using Wilcoxon t-test by pooling data across three genetically diverse biological replicates.

Visualization of live bacteria in the gut was carried out using *Bac*Light stains [66]. One milliliter of bacterial cultures grown overnight at RT were pelleted and washed twice with cASW and stained with 4 µl of *Bac*Light Red (Invitrogen Cat no B35001) for 15 mins in the dark. The stained cultures were then washed twice with cASW, and then

diluted to 10^7 cfu/ml with cASW. MS4 animals in 6-well dishes were then exposed to 5 ml of this culture. Bacteria in the gut of animals were visualized after 15 mins on a Leica DMI 6000B stereoscope with a CY5 fluorescent filter and imaged-captured with a Hamamatsu *Orca ii* camera (model C10600-10B-H) and processed with the MetaMorph 7.10.4 imaging suite (Molecular Devices, Downingtown PA).

Gene expression studies

To determine if the host immune system can recognize and respond to the unique sub-strains, which differ only in the presence or absence of the prophages, reverse transcription-quantitative PCR (RT-qPCR) was performed. RNA was extracted using the RNA XS kit (Macherey-Nagel, Düren, Germany) from MS4 *Ciona* juveniles that underwent gut colonization. Complementary DNA (cDNA) synthesis was performed with oligo-dT primers and random hexamers using the First Strand cDNA Synthesis Kit (Promega, Madison WI) following manufacturer's instructions. Amplification was set up with the qPCR kit (Promega, Madison, WI) and carried out on an ABI7500 with recommended reaction conditions. Targeted genes, and their primers, are reported in **Table *2*** Results from four distinct biological replicates are presented. Each replicate includes pooled *Ciona* juveniles from at least two wells of a 6-well dish. *Ciona* actin was referenced as an endogenous control. Data was analyzed using $\Delta\Delta C_T$ method [67] and the ABI7500 software suite.

Statistical analysis and data visualization

Statistical analysis and data visualization were carried out in R, version 4.2 [68]. Data were plotted with ggplot 3.3.5 [69]; the Beeswarm plot was constructed using ggbeeswarm 0.6 [70]. Beeswarm plots and statistics for motility assays were calculated using replicate averages [71]. Statistical significance was calculated using ggsignif package 0.6.3 or ggpubr0.4.0 [72, 73]. If the data were found to be normally distributed by Shapiro's test, then significance was calculated using an unpaired t-test. The Wilcoxon signed-rank test was used to calculate significance of non-parametric data.

Results

S. fidelis 3313 genome assembly

The *S. fidelis* 3313 genome assembly resulted in 34 contigs totaling 4,901,198 bp with a G+C content of 42.95%. These contigs represent the main genome assembly, spanning ~99.84% of the reference genome with only 0.04% possible contamination as evaluated by CheckM [47]. The two largest contigs (4,824,570 bp and 43,647 bp each) are predicted to encode 98.6% of the genome (**Figure 1**). Based on CompareM analysis, strain 3313 shares ~99% average amino acid identity with the *S. fidelis* ATCC BAA-318 isolate first identified in sediments of the South China Sea and ~93% of the genes are orthologous. Our previous size prediction of the two prophages, SfMu1 and SfPat (**Table 3**), included some adjacent bacterial genomic DNA, indicating SfMu1 to be 45,796 bp [36]. However, the current improved assemblies and PhiSpy predictions indicate a smaller size of 27,293 bp, which is consistent with sequenced DNA from mitomycin-C induced fractions. Homology of the integrase gene product supports

SfMu1 as a Mu-like phage [74]. Likewise, homology of the capsid proteins indicates that SfPat is a PM2-like phage [75]. These phages are localized to Contig 1 of the current assembly.

A third inducible 60,137 bp prophage, encoding 68 ORFs, was also identified in the improved genome assembly. This third prophage is predicted to be most closely related to the MuSo1 phage component of *Shewanella* FJAT-53749 (accession no. WP_220070840.1) based on similarity of its integrase, capsid protein and protease sequences. Additional prophage ORFs encoding proteins matching MuSo1 are described in **Table 4** and include structural proteins, terminase small unit (accession no. K0057259.1), terminase large unit (accession no WP_168825185.1), and the Mu-like flu mu region (accession no. KJE44690.1) homologous to Mu-like phage components **Table 4**. Because of its similarity to the Mu family of phage proteins, this prophage is termed SfMu2.

Additional sequence contigs that do not assemble to the main *S. fidelis* 3313 genome include at least three small contigs encoding potential phage ORFs. However, only three unique particle morphologies were observed under the transmission electron microscope (**Figure 1b-d**). Previous attempts to sequence mitomycin-C induced fractions were similarly only able to detect SfPat and Mu family phages [36].

Targeting prophages for deletion

To study the influence of prophages on *S. fidelis* 3313, we targeted two of the three prophages, SfPat and SfMu1, for deletion using homologous recombination. The third prophage, SfMu2, is quite large (over 65 kb) and is being targeted as part of future

efforts. To target SfMu1, primers EDK73/74 and EDK75/76 were designed to amplify 667 bp upstream and 752 bp downstream of the prophage (**Figure 2a**). Flanking primers EDK83/84 were used for PCR screening of candidate deletion clones, amplifying 1607 bp in the event of a successful deletion, and yielding no product in case of an unsuccessful deletion as the product is too large to amplify. To target SfPat, primers EDK77/78 and EDK79/80 were designed to amplify 773 bp upstream and 758 bp downstream of the prophage, respectively (**Figure 2b**). These upstream and downstream regions also contain the first 33 and last 95 bp, respectively, of SfPat. Flanking primers EDK81/82 were used for PCR screening of candidate colonies for SfPat deletion. The flanking primers produce a manageable product of 1697 bp in the event of a successful deletion, as the distance between the regions is vastly decreased by the lack of prophage. In the event of an unsuccessful deletion no product would be expected as the prophage spans over 10 kb between the flanking regions.

Colony PCR and single primer extension sequencing were both used to validate all deletions, using primers EDK81/82 for SfPat and EDK83/84 for SfMu1 (**Table 5**). All recovered amplicon sizes were consistent with predictions for both SfPat deletion and SFMu1 deletion (Fig 2c). The SfMu1 deletion strain was subsequently named JG4005 and the SfPat deletion was named JG3862. SfPat was further deleted from JG4005, establishing a double mutant, JG4063. The full genomes of all strains were re-sequenced by Illumina sequencing (MiGS, University of Pittsburgh) to confirm the absence of additional genetic changes or mutations in either the upstream or downstream flanking regions of the deletion mutants. The deletion mutants were then

used for *in vitro* and *in vivo* experiments to understand the potential role of prophages in shaping *S. fidelis* 3313 colonization dynamics in the gut of *Ciona.*

Prophage deletion modulates biofilm formation and motility in *S. fidelis* 3313

Deletion of prophage regions from *S. fidelis* 3313 contributed to an overall increase in biofilm formation as quantified by crystal violet staining (**Figure 3a**). Specifically, we observed that the strains possessing a SfPat deletion alone, or with deletion of both prophages (i.e., double mutant), demonstrate approximately 23% increased biofilm concentrations compared to wild type (WT) strains with a p-value of 0.026 and 0.028 respectively (**Figure 3a**). Conventionally, to form a biofilm bacteria will settle and initiate stationary growth dynamics [76]. To determine if the prophages were influencing motility in *S. fidelis* 3313 we studied bacterial swimming on simple semi-solid media motility assays by measuring the diameter of spread from a primary inoculation point after an overnight incubation as described above. WT strains demonstrated the largest mean diameter of 8.21 mm. The deletion of SfMu1 and SfPat resulted in decreased diameters of 5.79 mm and 4.04 mm, respectively. Deleting both the prophages resulted in the smallest diameter of 3.58 mm. Thus, strains with deleted prophages demonstrated reduced motility and increased biofilm formation compared to the WT (**Figure 3b**).

Since swimming and biofilm formation behaviors are dependent on quorum sensing mechanisms, we measured changes in the expression levels of *pdeB,* which encodes a phosphodiesterase that degrades cyclic-di-GMP and can serve as a negative regulator of motility, positive regulator of biofilm formation and a quorum sensing signal

[77]. Deletion of prophages has been shown previously to result in increased expression of *pdeB* in *S. oneidensis* [77]. Deletion of SfPat in *S. fidelis* 3313 resulted in a small but significant reduction in *pdeB* gene expression compared to the WT (p-value 0.033), while deletion of SfMu1 had an insignificant reduction in expression of *pdeB*. However, deletion of both prophages resulted in over two-fold down regulation of *pdeB* expression (p-value 0.001) compared to the WT (**Figure 3c**).

Prophages shape the outcome of *S. fidelis* 3313 colonization of the *Ciona* gut

Since motility and biofilm formation are typically critical to shaping bacterial communities, we investigated whether prophages could impact the ability of *S. fidelis* 3313 to colonize the *Ciona* gut. Colonization assays were performed on MS4 *Ciona* juveniles by exposing animals to individual strains as described above, repeating the experiments three times across juveniles with diverse genetic backgrounds, i.e., using gametes from distinct outbred adults harvested from southern California (M-Rep). Wildtype *S. fidelis* 3313 stained with *Bac*Light Red were observed in the gut of MS4 *Ciona* juveniles within 10 minutes of exposure (**Figure 4a**), revealing a rapid concentration of the strain into the gut compartments. The double KO strain also colonizes the gut (data not shown), but additional experiments are necessary to define if significant differences exist. One hour after exposure to the sub-strains, bacteria were recovered from animal guts and retention, i.e., colonization, was determined by counting colony forming units (cfus) (**Figure 4 b-d**). Retention of the double KO strain was 0.44-to-0.724-fold decreased compared to the WT strain. The SfPat KO revealed a statistically insignificant 1.3-to-1.5-fold increase in retention in all three rounds. The

SfMu1 KO colonized the gut with high variability. While these trends were consistent in individual rounds, they were not statistically significant (Wilcoxon test, **Figure 4e**) when cfu data were pooled across diverse genetic backgrounds.

Host immunity plays an important role in shaping gut homeostasis. Distinct microbes and their antigens and/or metabolites can modulate host immune responses [78]. To determine if host immunity discriminates among *S. fidelis* 3313 sub-strains, only differing in the presence or absence of prophages, we examined the expression patterns of a secreted immune effector, VCBP-C. Under normal healthy conditions, VCBP-C is expressed and secreted by the gut epithelium where it can bind (and opsonize) bacteria within the gut lumen [42] and influence biofilms *in vitro* [43]. After one hour of exposure, up-regulation of VCBP-C was observed in *Ciona* juveniles exposed to phage KO strains of *S. fidelis* 3313, compared to the WT strain (**Figure 4f**) by qPCR. A significant three-fold over expression (p-value 0.042) of VCBP-C was noted in *Ciona* exposed to the double KO, as compared to those exposed to the WT strain. Statistically significant two-fold increases in VCBP-C expression were also noted in *Ciona* juveniles exposed to the individual phage KOs compared to WT.

Discussion

In this study, a nearly completed genome of *S. fidelis* 3313 is provided by combining short- (Illumina sequencing) and long-read assemblies (PacBio sequencing), resulting in improved localization of two known prophages, SfPat and SfMu1. A third prophage, SfMu2, was also identified and its genomic location recognized here. SfPat and SfMu1 were deleted via homologous recombination approaches and the resulting sub-strains

studied to determine the impact of prophages on colonization dynamics. We report that prophages are impacting important phenotypes of *S. fidelis* 3313. For example, prophage KO led to reduced motility and corresponding increases in biofilm formation in 24-hour cultures. SfPat single-KO strains revealed more significant phenotypes compared to SfMu1 single-KO strains, while double-KO strains revealed the largest changes.

Biofilm formation and motility are often regulated by secondary signaling molecules like cyclic-di-GMP [79]. To determine if prophages of *S. fidelis* 3313 shape these traits by modulating cyclic-di-GMP levels, we monitored changes to the levels of an important regulatory enzyme of this dinucleotide. The phosphodiesterase PdeB is a known negative regulator of cyclic-di-GMP and its expression have been shown to influence biofilm formation and motility in *S. oneidensis* [77]. We report that deletion of prophages in *S. fidelis* 3313 results in decreased expression of *pdeB* in KO strains compared to the WT during colonization of MS4 *Ciona* juveniles. This likely results in an increase in the accumulation of cyclic-di-GMP in the double KO strain. Based on these results, we hypothesize that increased cyclic-di-GMP in the prophage KO strains leads to reduced motility and increased biofilm formation. Increased cyclic-di-GMP levels have also been reported to reduce motility and impact biofilm morphology in *Vibrio fischeri* [80]. It has also been reported that the influence of a *Vibrio anguillarum* prophage is repressed by specific quorum sensing mechanisms and that this action results in an increase in biofilm formation [81]. Some prophages have also been shown to contain other genes that are responsible for shaping motility of *Pseudomonas aeruginosa* [82]. In this report, we find that prophages of *S. fidelis* 3313 do not appear to significantly

influence colonization dynamics in the gut of *Ciona*, as measured by comparing retention of live bacteria. However, the impact of prophages on host colonization may be obscured by the influence of host genetics as suggested by differential retention rates across genetic backgrounds (**Figure 4**). Similarly, it was recently reported that the marine phage, HLN01, has no apparent influence on how the bacterial symbiont, *Vibrio fischeri*, colonizes its natural host, the bobtail squid *Euprymna scolopes* [83].

Previously, secretory immunoglobulin A (SIgA) of humans was found to enhance and favor settlement dynamics of bacteria both *in vitro* and *in vivo* [84-87], raising a basic question as to whether this phenomenon is more widespread among other secretory immune effectors present in mucosal environments of animals [88]. We speculate that while prophages likely impact the behavior of lysogenized bacteria in ways that can influence colonization dynamics, interaction with VCBP-C on the mucosal surface of the *Ciona* gut may subsequently influence settlement behaviors [43, 88]. Importantly, we show here that loss of prophages, e.g., the KO sub-strains, results in increased expression of VCBP-C. It remains to be shown if prophages stimulate the production of a bacterial metabolite with immunomodulatory properties, or if the host immune system is responding to differences in bacterial behaviors or traits that result from absence of the prophage influence, e.g., excess biofilm formation.

Metagenomic sequencing of gut microbes from healthy animals has revealed that temperate lifestyles are prevalent among phages from these ecosystems [89-91], an observation also made in the *Ciona* gut [17]. Various environmental triggers such as UV light and chemical agents like mitomycin C (a known mutagen) have been shown to induce a switch from the lysogenic to lytic cycle via the SOS response, a cell-wide

response to DNA damage that can promote survival [92]. However, SOS-independent stressors such as antibiotics [19, 27] as well as local inflammation [21] also induce prophages, which can result in lysis and the release of viral particles, which may target related bacteria and disrupt homeostasis in mucosal environments. Yet, it remains unclear how temperate lifestyles shape colonization behaviors among gut bacteria. While the data reported here are only based on one bacterial strain that colonizes the *Ciona* gut, we find that lysogenized versions of *S. fidelis* colonize the gut with reduced activation of VCBP-C gene expression. These observations may be more widely applicable since lysogens are so abundant in animal microbiomes. While VCBP-C may shape settlement dynamics, it is produced normally in copious amounts so that chitin-rich mucus of the gut is close to saturated with the secreted immune effector, as revealed by immunohistochemical staining [43]. Therefore, overexpression of VCBP-C is not necessarily helpful and often corresponds to other induced inflammatory responses.

VCBPs, which undoubtedly possess broad specificities, can bind a range of bacterial hosts, however, it remains unclear if they bind lysogenized bacteria with different affinities than their prophage-free counterparts. Since colonization of animal mucosal surfaces is an ancient process [35], it is likely that prophages and their integration into bacterial genomes have evolved to provide fitness benefits in these often-challenging environments. Determining the role animal immunity plays in these exchanges will be of broad interest. Beyond the indication that prophages can be induced to generate lytic particles with the capacity to influence the structure of the microbiome, serve as an indirect form of protection for the host [26, 93, 94], and/or

contribute to the transfer of virulence factors [25, 95], it is likely that their role in shaping colonization dynamics is prioritized if it provides fitness benefits to the lysogenized bacteria. Future studies should clarify the relationship between secreted immune effectors and lysogenized bacteria in processes shaping settlement dynamics, while providing significant direction in gaining a broader understanding of the microbiome and the multifactorial nature of homeostasis.

Author contributions

O.N. designed, executed, and analyzed experiments and wrote and edited the manuscript, S.L.G., N.P., C.G.F.A., B.A.L., A.L., and E.D.K performed experiments and provided feedback and approved the manuscript, M.N.Y., S.J.L., and B.A.L. performed genome sequence analysis, assembly, and provided feedback and approved the manuscript, M.B. helped interpret data, provided feedback and approved the manuscript, G.A.L. provided reagents, helped design deletion experiments, helped interpret data, and provided feedback and approved the manuscript, and L.J.D. funded most of the project, helped design experiments, interpret data, and helped write, edit, and approved the final version of the manuscript.

Funding

This project was supported by NSF IOS 1456301 (L.J.D. and M.B.) and NSF MCB 1817308 and internal awards from the MCOM Deans Office and the USF Institute for Microbiomes to L.J.D., an NSF GRFP award to B.A.L., and a New Investigator Award to O.N.

Acknowledgments

The authors would like to acknowledge the expert technical assistance of Anthony Greco and Amanda Garces for transmission electron microscopy, and Gary Litman, John Cannon for expert feedback and guidance in early efforts of the project.

References

1. Li, H., et al., *The outer mucus layer hosts a distinct intestinal microbial niche.* Nat Commun, 2015. **6**: p. 8292.
2. Johansson, M.E., J.M. Larsson, and G.C. Hansson, *The two mucus layers of colon are organized by the MUC2 mucin, whereas the outer layer is a legislator of host-microbial interactions.* Proc Natl Acad Sci U S A, 2011. **108 Suppl 1**: p. 4659-65.
3. Duncan, K., K. Carey-Ewend, and S. Vaishnava, *Spatial analysis of gut microbiome reveals a distinct ecological niche associated with the mucus layer.* Gut Microbes, 2021. **13**(1): p. 1874815.

4. Harrington, V., et al., *Ecology and medicine converge at the microbiome-host interface.* mSystems, 2021: p. e0075621.
5. Hornung, B., et al., *Studying microbial functionality within the gut ecosystem by systems biology.* Genes Nutr, 2018. **13**: p. 5.
6. Moran, N.A., H. Ochman, and T.J. Hammer, *Evolutionary and ecological consequences of gut microbial communities.* Annu Rev Ecol Evol Syst, 2019. **50**(1): p. 451-475.
7. Mirzaei, M.K. and C.F. Maurice, *Ménage à trois in the human gut: interactions between host, bacteria and phages.* Nature Reviews Microbiology, 2017. **15**(7): p. 397-408.
8. Shkoporov, A.N. and C. Hill, *Bacteriophages of the human gut: the "known unknown" of the microbiome.* Cell Host & Microbe, 2019. **25**(2): p. 195-209.
9. Howard-Varona, C., et al., *Lysogeny in nature: mechanisms, impact and ecology of temperate phages.* ISME J, 2017. **11**(7): p. 1511-1520.
10. Lwoff, A., *Lysogeny.* Bacteriological Reviews, 1953. **17**(4): p. 269-337.
11. Boling, L., et al., *Dietary prophage inducers and antimicrobials: toward landscaping the human gut microbiome.* Gut Microbes, 2020. **11**(4): p. 721-734.
12. Mills, S., et al., *Movers and shakers: influence of bacteriophages in shaping the mammalian gut microbiota.* Gut Microbes, 2013. **4**(1): p. 4-16.
13. Bondy-Denomy, J. and A.R. Davidson, *When a virus is not a parasite: the beneficial effects of prophages on bacterial fitness.* J Microbiol, 2014. **52**(3): p. 235-242.
14. Aziz, R.K., et al., *Mosaic prophages with horizontally acquired genes account for the emergence and diversification of the globally disseminated M1T1 clone of Streptococcus pyogenes.* J Bacteriol, 2005. **187**(10): p. 3311-3318.
15. Jiang, S.C. and J.H. Paul, *Significance of lysogeny in the marine environment: studies with isolates and a model of lysogenic phage production.* Microb Ecol, 1998. **35**(3): p. 235-243.
16. Silveira, C.B., A. Luque, and F. Rohwer, *The landscape of lysogeny across microbial community density, diversity and energetics.* Environ Microbiol, 2021. **23**(8): p. 4098-4111.
17. Leigh, B.A., et al., *The gut virome of the protochordate model organism, Ciona intestinalis subtype A.* Virus Res, 2018. **244**: p. 137-146.
18. Kim, M.-S. and J.-W. Bae, *Lysogeny is prevalent and widely distributed in the murine gut microbiota.* ISME J, 2018. **12**(4): p. 1127-1141.
19. Allen, H.K., et al., *Antibiotics in feed induce prophages in swine fecal microbiomes.* MBio, 2011. **2**(6).
20. Banks, D.J., B. Lei, and J.M. Musser, *Prophage induction and expression of prophage-encoded virulence factors in group A Streptococcus serotype M3 strain MGAS315.* Infect Immun, 2003. **71**(12): p. 7079-86.
21. Diard, M., et al., *Inflammation boosts bacteriophage transfer between Salmonella spp.* Science, 2017. **355**(6330): p. 1211-1215.
22. Fang, Y., et al., *Induction of shiga toxin-encoding prophage by abiotic environmental stress in food.* Appl Environ Microbiol, 2017. **83**(19).
23. Garcia-Russell, N., B. Elrod, and K. Dominguez, *Stress-induced prophage DNA replication in Salmonella enterica serovar Typhimurium.* Infect Genet Evol, 2009. **9**(5): p. 889-95.
24. Maiques, E., et al., *beta-lactam antibiotics induce the SOS response and horizontal transfer of virulence factors in Staphylococcus aureus.* J Bacteriol, 2006. **188**(7): p. 2726-9.
25. Nanda, A.M., K. Thormann, and J. Frunzke, *Impact of spontaneous prophage induction on the fitness of bacterial populations and host-microbe interactions.* J Bacteriol, 2015. **197**(3): p. 410-9.

26. Wang, X., et al., *Cryptic prophages help bacteria cope with adverse environments.* Nat Commun, 2010. **1**: p. 147.
27. Zhang, X., et al., *Quinolone antibiotics induce Shiga toxin-encoding bacteriophages, toxin production, and death in mice.* J Infect Dis, 2000. **181**(2): p. 664-70.
28. Fortier, L.C. and O. Sekulovic, *Importance of prophages to evolution and virulence of bacterial pathogens.* Virulence, 2013. **4**(5): p. 354-65.
29. Hu, J., et al., *Prophage activation in the intestine: insights into functions and possible applications.* Front Microbiol, 2021. **12**: p. 785634.
30. Lin, W., et al., *Identification of a Vibrio cholerae RTX toxin gene cluster that is tightly linked to the cholera toxin prophage.* Proc Natl Acad Sci U S A, 1999. **96**(3): p. 1071-1076.
31. Swidsinski, A., et al., *Comparative study of the intestinal mucus barrier in normal and inflamed colon.* Gut, 2007. **56**(3): p. 343-50.
32. Liu, X., et al., *Physiological function of Rac prophage during biofilm formation and regulation of Rac excision in Escherichia coli K-12.* Sci Rep, 2015. **5**(1): p. 16074.
33. Rice, S.A., et al., *The biofilm life cycle and virulence of Pseudomonas aeruginosa are dependent on a filamentous prophage.* ISME J, 2009. **3**(3): p. 271-282.
34. Gödeke, J., et al., *Phage-induced lysis enhances biofilm formation in Shewanella oneidensis MR-1.* ISME J, 2011. **5**(4): p. 613-626.
35. Dishaw, L.J., et al., *The gut of geographically disparate Ciona intestinalis harbors a core microbiota.* PLoS One, 2014. **9**(4): p. e93386.
36. Leigh, B., et al., *Isolation and characterization of a Shewanella phage–host system from the gut of the tunicate, Ciona intestinalis.* Viruses, 2017. **9**(3): p. 60.
37. Chiba, S., et al., *Development of Ciona intestinalis juveniles (through 2nd ascidian stage).* Zoolog Sci, 2004. **21**(3): p. 285-98.
38. Davidson, B., *Ciona intestinalis as a model for cardiac development.* Semin.Cell Dev.Biol, 2007. **18**(1): p. 16-26.
39. Liu, L.-P., et al., *Ciona intestinalis as an emerging model organism: Its regeneration under controlled conditions and methodology for egg dechorionation.* J. Zhejiang Univ. Sci. B, 2006. **7**(6): p. 467-474.
40. Liberti, A., et al., *Reflections on the use of an invertebrate chordate model system for studies of gut microbial immune interactions.* Front Immunol, 2021. **12**.
41. Liberti, A., et al., *A soluble immune effector binds both fungi and bacteria via separate functional domains.* Front Immunol, 2019. **10**: p. 369.
42. Dishaw, L.J., et al., *A role for variable region-containing chitin-binding proteins (VCBPs) in host gut–bacteria interactions.* Proc Natl Acad Sci U S A, 2011. **108**(40): p. 16747-16752.
43. Dishaw, L.J., et al., *Gut immunity in a protochordate involves a secreted immunoglobulin-type mediator binding host chitin and bacteria.* Nat Commun, 2016. **7**: p. 10617.
44. Liu, X., et al., *Symbiosis of a P2-family phage and deep-sea Shewanella putrefaciens.* Environ Microbiol, 2019. **21**(11): p. 4212-4232.
45. Bolger, A.M., M. Lohse, and B. Usadel, *Trimmomatic: a flexible trimmer for Illumina sequence data.* Bioinformatics, 2014. **30**(15): p. 2114-20.
46. Wick, R.R., et al., *Unicycler: resolving bacterial genome assemblies from short and long sequencing reads.* PLoS Comp Biol, 2017. **13**(6): p. e1005595.
47. Parks, D.H., et al., *CheckM: assessing the quality of microbial genomes recovered from isolates, single cells, and metagenomes.* Genome Res, 2015. **25**(7): p. 1043-55.
48. Parks, D., *CompareM: Comparative Genomic Statistics*. 2020: github.
49. Aziz, R.K., et al., *The RAST server: rapid annotations using subsystems technology.* BMC Genomics, 2008. **9**(1): p. 75.

50. Akhter, S., R.K. Aziz, and R.A. Edwards, *PhiSpy: a novel algorithm for finding prophages in bacterial genomes that combines similarity- and composition-based strategies.* Nucleic Acids Res, 2012. **40**(16): p. e126-e126.
51. Kieft, K., Z. Zhou, and K. Anantharaman, *VIBRANT: automated recovery, annotation and curation of microbial viruses, and evaluation of viral community function from genomic sequences.* Microbiome, 2020. **8**(1).
52. Roux, S., et al., *VirSorter: mining viral signal from microbial genomic data.* PeerJ, 2015. **3**: p. e985.
53. Arndt, D., et al., *PHASTER: a better, faster version of the PHAST phage search tool.* Nucleic Acids Res, 2016. **44**(W1): p. W16-W21.
54. Saltikov, C.W. and D.K. Newman, *Genetic identification of a respiratory arsenate reductase.* Proc Natl Acad Sci U S A, 2003. **100**(19): p. 10983-10988.
55. Bryksin, A.V. and I. Matsumura, *Overlap extension PCR cloning: a simple and reliable way to create recombinant plasmids.* BioTechniques, 2010. **48**(6): p. 463-465.
56. Cochran, P., C. Kellogg, and J. Paul, *Prophage induction of indigenous marine lysogenic bacteria by environmental pollutants.* Marine Ecol Prog Ser, 1998. **164**: p. 125-133.
57. Hurwitz, B.L., et al., *Evaluation of methods to concentrate and purify ocean virus communities through comparative, replicated metagenomics.* Environ Microbiol, 2013. **15**(5): p. 1428-1440.
58. Ackermann, H.-W. and M. Heldal, *Basic electron microscopy of aquatic viruses.* Manual of Aquatic Viral Ecology, 2010. **18**: p. 182-192.
59. Liberti, A., et al., *A Role for Secreted Immune Effectors in Microbial Biofilm Formation Revealed by Simple In Vitro Assays*, in *Immune Receptors: Methods and Protocols*, J. Rast and K. Buckley, Editors. 2022, Springer US: New York, NY. p. 127-140.
60. Wolfe, A.J. and H.C. Berg, *Migration of bacteria in semisolid agar.* Proc Natl Acad Sci U S A, 1989. **86**(18): p. 6973-7.
61. Kearns, D.B., *A field guide to bacterial swarming motility.* Nat Rev Microbiol, 2010. **8**(9): p. 634-44.
62. Cirino, P., et al., *Laboratory culture of the ascidian Ciona intestinalis (L.): a model system for molecular developmental biology research*, in *Mar. Mod. Elec. Rec. [serial online]*. 2002.
63. Leigh, B.A., A. Liberti, and L.J. Dishaw, *Generation of germ-free Ciona intestinalis for studies of gut-microbe interactions.* Front Microbiol, 2016. **7**: p. 2092.
64. Gaudy Jr, A., F. Abu-Niaaj, and E. Gaudy, *Statistical study of the spot-plate technique for viable-cell counts.* Appl Microbiol, 1963. **11**(4): p. 305-309.
65. Miles, A.A., S. Misra, and J. Irwin, *The estimation of the bactericidal power of the blood.* Epidemiol Infecti, 1938. **38**(6): p. 732-749.
66. Boulos, L., *Pré vost M, Barbeau B, Coallier J, Desjardins R. LIVE/DEAD BacLight: application of a new rapid staining method for direct enumeration of viable and total bacteria in drinking water.* J Microbiol Methods, 1999. **37**: p. 77-86.
67. Pfaffl, M.W., *A new mathematical model for relative quantification in real-time RT-PCR.* Nucleic Acids Res, 2001. **29**(9): p. e45.
68. Team, R.C., *R : A language and environment for statistical computing.* 2021.
69. Wickham, H., *ggplot2: Elegant Graphics for Data Analysis*. 2016.
70. Eklund, A.T., James, *The Bee Swarm Plot, an Alternative to Stripchart*. 2021: github.
71. Lord, S.J., et al., *SuperPlots: Communicating reproducibility and variability in cell biology.* J Cell Biol, 2020. **219**(6): e202001064.
72. Kassambara, A., *ggpubr: 'ggplot2' Based Publication Ready Plots*. 2020: github.
73. Constantin, A.-E.P., Indrajeet, *{ggsignif}: R Package for Displaying Significance Brackets for {'ggplot2'}*. 2021: PsyArxiv.
74. Harshey, R.M., *Phage Mu*. 1988, Springer US. p. 193-234.

75. Männistö, R.H., et al., *The complete genome sequence of PM2, the first lipid-containing bacterial virus to be isolated.* Virology, 1999. **262**(2): p. 355-363.
76. Watnick, P. and R. Kolter, *Biofilm, city of microbes.* J Bacteriol, 2000. **182**(10): p. 2675-2679.
77. Chao, L., et al., *PdeB, a cyclic di-GMP-specific phosphodiesterase that regulates Shewanella oneidensis MR-1 motility and biofilm formation.* J Bacteriol, 2013. **195**(17): p. 3827-3833.
78. Rooks, M.G. and W.S. Garrett, *Gut microbiota, metabolites and host immunity.* Nature Rev Immunol, 2016. **16**(6): p. 341-352.
79. Jenal, U. and J. Malone, *Mechanisms of cyclic-di-GMP signaling in bacteria.* Ann Rev Genetics, 2006. **40**(1): p. 385-407.
80. Isenberg, R.Y., et al., *High levels of cyclic diguanylate interfere with beneficial bacterial colonization.* Mbio, 2022. **13**(4): p. e01671-22.
81. Tan, D., et al., *High cell densities favor lysogeny: induction of an H20 prophage is repressed by quorum sensing and enhances biofilm formation in Vibrio anguillarum.* ISME J, 2020. **14**(7): p. 1731-1742.
82. Tsao, Y.-F., et al., *Phage morons play an important role in Pseudomonas aeruginosa phenotypes.* J Bacteriol, 2018. **200**(22): p. e00189-18.
83. Lynch, J.B., et al., *Independent host- and bacterium-based determinants protect a model symbiosis from phage predation.* Cell Reports, 2022. **38**(7): p. 110376.
84. Bollinger, R.R., et al., *Secretory IgA and mucin-mediated biofilm formation by environmental strains of Escherichia coli: role of type 1 pili.* Mol Immunol, 2006. **43**(4): p. 378-87.
85. Thomas, A.D. and W. Parker, *Cultivation of epithelial-associated microbiota by the immune system.* Future Microbiol, 2010. **5**(10): p. 1483-92.
86. Pratt, L.A. and R. Kolter, *Genetic analysis of Escherichia coli biofilm formation: roles of flagella, motility, chemotaxis and type I pili.* Mol Microbiol, 1998. **30**(2): p. 285-93.
87. Donaldson, G.P., et al., *Gut microbiota utilize immunoglobulin A for mucosal colonization.* Science, 2018. **360**(6390): p. 795-800.
88. Dishaw, L.J., et al., *Immune-directed support of rich microbial communities in the gut has ancient roots.* Dev Comp Immunol, 2014.
89. Minot, S., et al., *The human gut virome: inter-individual variation and dynamic response to diet.* Genome Res, 2011. **21**(10): p. 1616-25.
90. Minot, S., et al., *Rapid evolution of the human gut virome.* Proc Natl Acad Sci U S A, 2013. **110**(30): p. 12450-5.
91. Reyes, A., et al., *Viruses in the faecal microbiota of monozygotic twins and their mothers.* Nature, 2010. **466**(7304): p. 334-8.
92. Weinbauer, M.G. and C.A. Suttle, *Lysogeny and prophage induction in coastal and offshore bacterial communities.* Aquat Microb Ecol, 1999. **18**(3): p. 217-225.
93. Barr, J.J., et al., *Bacteriophage adhering to mucus provide a non-host-derived immunity.* Proc Natl Acad Sci U S A, 2013. **110**(26): p. 10771-6.
94. Wang, X., et al., *Cryptic prophages help bacteria cope with adverse environments.* Nature Commun, 2010. **1**(1): p. 147.
95. Wagner, P.L. and M.K. Waldor, *Bacteriophage control of bacterial virulence.* Infect Immun, 2002. **70**(8): p. 3985-93.
96. Liberti, A., et al., *Chitin protects the gut epithelial barrier in a protochordate model of DSS-induced colitis.* Biology Open, 2018. **7**(1).

Figure Legends

Table 1: Strain list: All *S. fidelis* 3313 strains are submitted under the BioProject PRJNA903273 on NCBI

Organism	Phenotype	Biosample	Accession no
JG 4066	WT	SAMN317993881	JAPMLD000000000
JG4005	ΔSfMu1	SAMN317993882	JAPMLC000000000
JG3862	ΔSfPat	SAMN317993883	JAPMLB000000000
JG4063	ΔSfMu1ΔSfPat	SAMN317993884	JAPMLA000000000

Table 2 : Genes targeted and the necessary reverse transcription- qPCR primers.

Gene	Function	Genbank accession no.	Primer (5'-3')	Reference
VCBP-C-Fwd	Secreted immune effector in the gut	HQ324151	AGACCAACGCCAACACAGTA	[96]
VCBP-C-Rev			CCCATACATTGCAGCATTTC	
Actin–Fwd	Cytoskeletal actin Reference gene	AJ297725	CCCAAATCATGTTCGAAACC	[96]
Actin-Rev			ACACCATCACCACTGTCGAA	
pdeB-Fwd	Phophodiesterase		GCATCAGGGCTCTTACCAATAG	This study
pdeB-Rev			GAGGCGGTGATCCTTACAGATA	
RecA-Fwd	Recombinase – Bacterial Reference gene		CGTAGTGGTGCGGTAGATGT	This study
RecA-Rev			CGCATTGCTTGGCTCATCAT	

Table 3: Identification of prophages in *S. fidelis* 3313 genome

Phage	Contig	Range Start	Range End	Length (bp)	Proteins (number)	Phage type identity (Region showing identity)
SfMu2	1	1630281	1690417	60137	68	Mu (MuSo1)
SfPat	1	2100478	2116061	15584	34	PM2 or unclassified Corticovirus
SfMu1	1	3996436	4023728	27293	21	Mu

722 **Table 4:** SfMu2 Prophage protein identity

SfMu2 protein	BLAST related protein	Organism	Query cover	Percent identity	E value	Accession no
Integrase	Mu transposase C-terminal domain-containing protein - DNA binding protein	*Shewanella* sp. FJAT-53749	100	81.88	0	WP_220070840.1
MuSo1, transcriptional regulator, Cro/CI family	XRE family transcriptional regulator	*Shewanella hanedai*	87	55.8	2.00E-69	WP_144041017.1
MuSo1, transcriptional regulator, Cro/CI family	LexA family transcriptional regulator	*Aeromonas*	96	43.61	2.00E-63	WP_201978113.1
Transcriptional regulator of N-acetylglucosamine utilization, AraC family	AraC family transcriptional regulator	*Shewanella halifaxensis*	100	98.97	0	WP_108946816.1
Replication initiation ATPase; bacteriophage DNA transposition B protein	prophage MuSo1, DNA transposition protein, putative	*Shewanella baltica* OS625	94	50.65	5.00E-74	EHC04434.1
Replication initiation ATPase; bacteriophage DNA transposition B protein	transposase	*Shewanella algae*	73	68.89	3.00E-86	BCV29228.1
prophage MuSo1, positive regulator of late transcription	transcriptional regulator	*Shewanella* sp. FJAT-53749	88	95.65	8.00E-91	WP_220070849.1
Phage terminase, small subunit	Mu-like prophage FluMu protein gp27	*Rheinheimera* sp. KL1	93	65.43	9.00E-79	KOO57259.1
Phage terminase, large subunit	Phage Terminase	*Shewanella oncorhynchi*	98	88.59	0	WP_168825185.1
Mu-like prophage FluMu protein gp29	Mu-like prophage FluMu protein gp29	*Thalassomonas viridans*	96	0	55.17	KJE44690.1

Phage (Mu-like) virion morphogenesis protein	Phage Minor head protein	*Shewanella abyssi*	100	0	86.16	WP_248979124.1
Putative virion morphogenesis protein	phage virion morphogenesis protein	*Shewanella sp. 1CM18E*	99	86.45	3.00E-87	WP_248469180.1
prophage MuSo1, protein Gp32, putative	phage protease	*Shewanella sp*. FJAT-53749	100	0	82.56	WP_220070866.1
Phage major capsid protein	Mu-like prophage major head subunit gpT family protein	*Shewanella abyssi*	100	0	89.43	WP_248979132.1

Table 5: Primer sequences used in generation of prophage knockouts

EDK 73	SeaSq. phage cont. 7 del. Up Fw BamHI	AAACGGATCC AAGAGTTACTAGTGGCGTTTG
EDK 74	SeaSq. phage cont. 7 del. Up rev OEPCR	CAAGCTCAAG CCAGTCAAATCAAAGGTAGGT
EDK 75	SeaSq. phage cont. 7 del. Down Fw OEPCR	ATTTGACTGG CTTGAGCTTGTGAACATCG
EDK 76	SeaSq. phage cont. 7 del. Down rev SacI	ACACGAGCTC AAGTTCTGCCAAGTCGTAGG
EDK 77	SeaSq. phage cont. 6 del. Up Fw BamHI	AAATGGATCC CGATCAGCCTGCTAGTTTATT
EDK 78	SeaSq. phage cont. 6 del. Up rev OEPCR	ACGGAATAGG TTGAATGCGACTCAGGC
EDK 79	SeaSq. phage cont. 6 del. Down Fw OEPCR	TCGCATTCAA CCTATTCCGTCATGTTTAGCC
EDK 80	SeaSq. phage cont. 6 del. Down rev SacI	ACATGAGCTC GATGCAGATAAAGAGCCGTAAA
EDK 81	SeaSq. phage cont. 6 del. check fw	GTTTATTTTGTGGCAATCGCA
EDK 82	SeaSq. phage cont. 6 del. check rev	GGTAGCAGTGCTTAAACGAT
EDK 83	SeaSq. phage cont. 7 del. check fw	AAAAGTGAAGCAGGTCAAGG
EDK 84	SeaSq. phage cont. 7 del. check rev	GACAGGGCAACTTCAACAAG

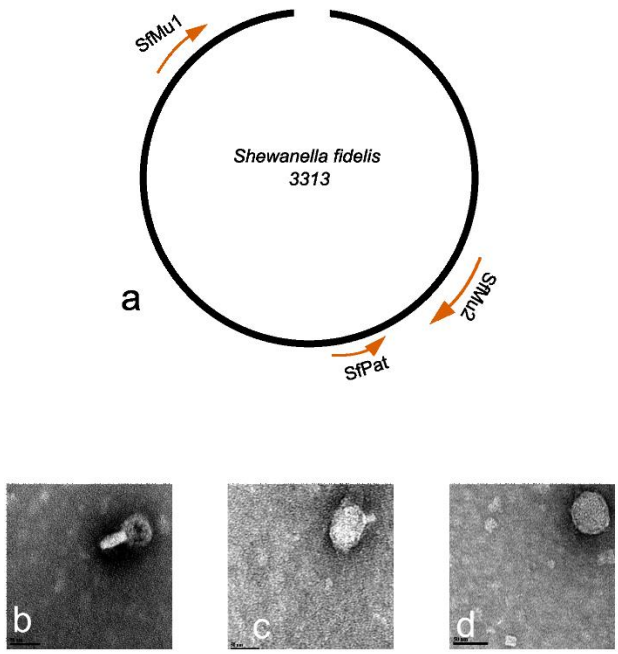

Figure 1. a) Schematic representation of the *S. fidelis* 3313 genomes to illustrate the relative positions of each prophage. (b-d) TEM images of phages identified from mitomycin-C induced *S. fidelis*, b) Myoviridae, c) Podoviridae, d) Corticoviridae

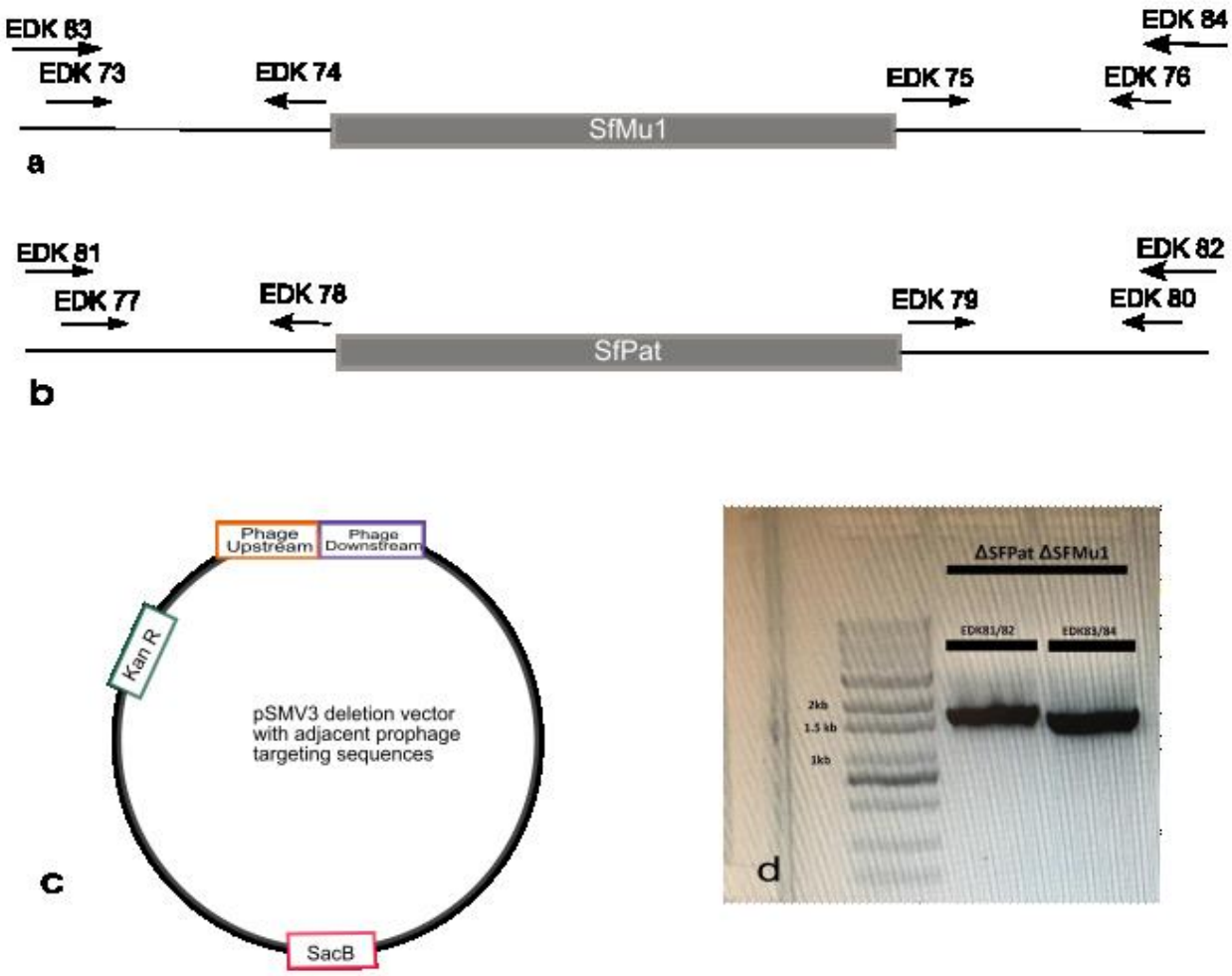

Figure 2. Prophage deletion from *Shewanella fidelis* 3313, a) Location of upstream, downstream and flanking primers that aid in deletion of SfMu1, b) Location of upstream, downstream and flanking primers that aid in deletion of SfPat, cc) pSMV3 suicide vector used for deletion of prophages showing flanking regions of the prophage used for deletion, and d) Flanking primers confirming the deletion of SfPat and SfMu1 on the prophage double knockout.

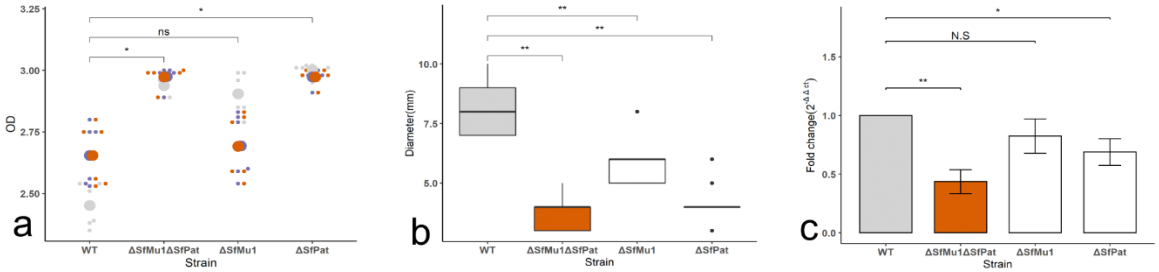

Figure 3. Deletion of prophage regions alter biofilm and motility in *S. fidelis* 3313, a) Strain with double prophage KO reveled higher biofilm formation after 24 hrs than the WT (n=3), b) WT revealed higher motility than the prophage deletion variants (n=6), and c) Fold change of *pdeB* with *RecA* as internal control from stage 4 juveniles of *Ciona* exposed to different prophage KO variants for one hour (n=4). *= p-value<0.05, **= p-value<0.01

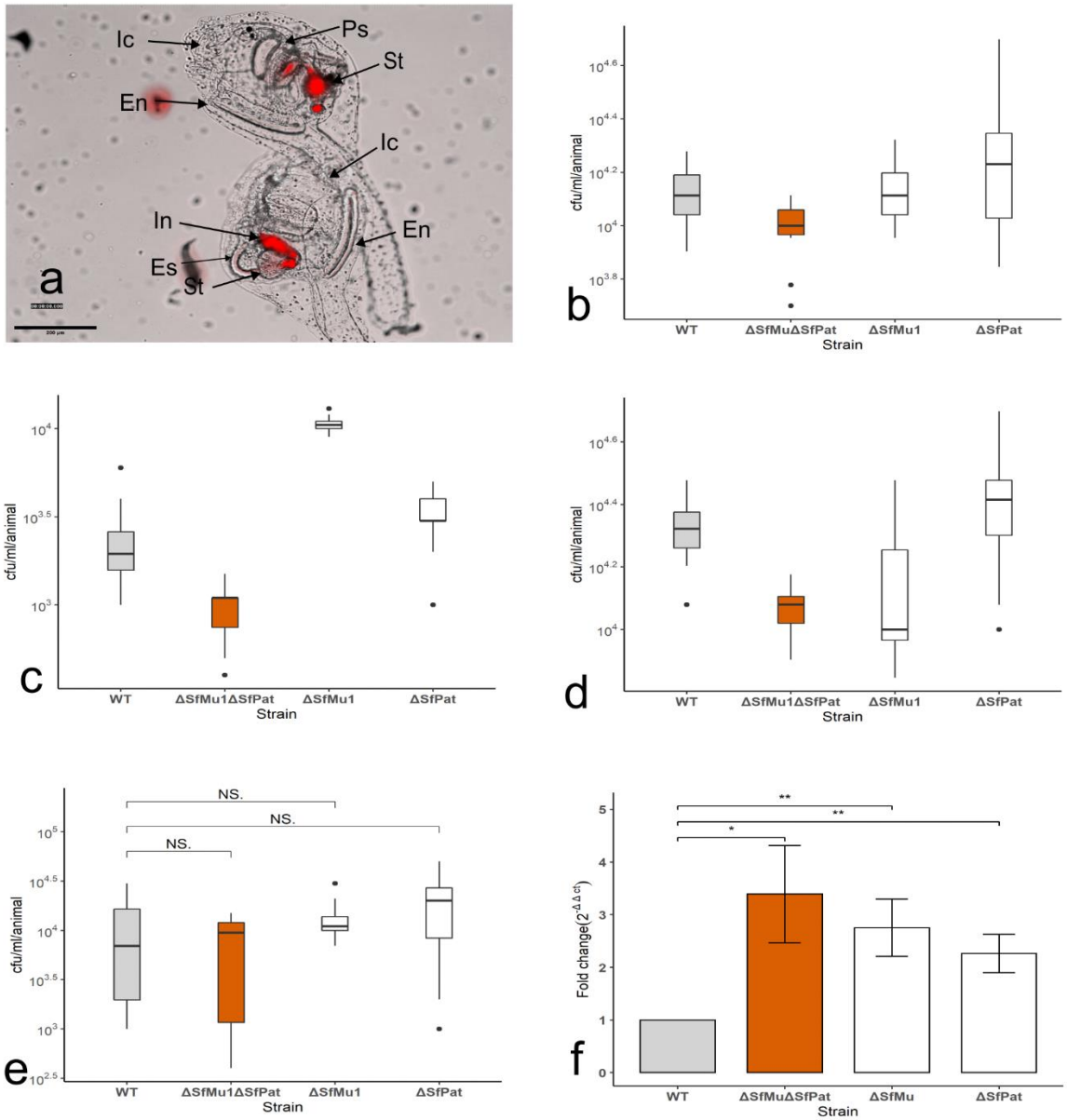

Figure 4. Prophages influence *S. fidelis* 3313 colonization of the gut and VCBP gene expression, a) *S. fidelis* 3313 stained with *Bac*Light Red is concentrated into the gut lumen in stage 4 *Ciona* juvenile after only 10 mins of exposure, (b-d) Three biological replicates of bacterial colonization from stage 4 juveniles exposed to prophage KO variants for one hour, e) Pooled rounds of three biological replicates where no significance is observed for gut colonization, and f) Fold change of VCBP-C with actin as an internal control from stage 4 juveniles of *Ciona* exposed to prophage KO variants for one hour (n=4). *= p-value<0.05, **= p-value<0.01. Ic=Incurrent siphon, En= Endostyle, Ps= Protostigmata, St= Stomach, In= Intestine.